J Mater Sci (2010) 45:1307–1314
DOI 10.1007/s10853-009-4083-6

Self-assembly of coordination polymers constructed from CuCN and unidentate pyridine bases

Safaa El-din H. Etaiw · Said A. Amer · Mohamed M. El-bendary

Received: 14 September 2009 / Accepted: 24 November 2009 / Published online: 11 December 2009

Abstract The self-assembly of $K_3[Cu(CN)_4]$ and unidentate pyridine bases (L): pyridine (py), 3-methyl pyridine (3-mpy), and 2,4,6-trimethyl pyridine (tmpy) in the presence of Me_3SnCl affords new coordination polymers (CPs) CuCN·0.5(py)] (**1**), [CuCN·0.5(3-mpy)] (**2**), and [CuCN·0.5(tmpy)] (**3**). The syntheses are achieved in H_2O/acetonitrile media at room temperature. The structure of the CP **3** was characterized by X-ray single crystal analysis. It is crystallized as orthorhombic in the space group Pnma, $a = 9.1065$ (3) Å, $b = 8.6669$ (3) Å, and $c = 12.1998$ (5) Å and $Z = 8$. The CPs **1**, **2** were investigated by IR, mass, Uv–visible, and ^{1}H-NMR spectra, as well as TGA. The CPs **1–3** are 2D-polymers consisting of 1D-$(CuCN)_n$ chain structure while the ligands alternate on both sides of the chain with associated copper atom coordination number of three. Hydrogen bonds play an essential role for developing 2D-network structure. These CPs exhibit strong fluorescent emissions in the solid state.

Introduction

Bottom-up construction of metal–organic frameworks (MOFs), possessing desired structure and bulk nature, from selected metals and organic ligand, is the central mission of crystal engineering [1–5]. As preparation of this practice, rational design of the structures of MOFs formed by self assembly has drawn considerable attention of current studies not only by biochemists but also by chemists interested in areas of modern synthetic chemistry that has been thoroughly surveyed by reviews [3, 6, 7].

S. E. H. Etaiw (✉) · S. A. Amer · M. M. El-bendary
Faculty of Science, Chemistry Department, Tanta University, Tanta, Egypt
e-mail: Safaaetaiw@hotmail.com

For Instance, a number of complexes of copper(I) cyanide have been reported over the years [8–14], but recent studies [15–18] have shown that there is still much to be learnt about such systems. The structure and the properties of copper(I) cyanide itself have been the subject of a number of studies over the years [19–25]. The most recently reported results show that solid CuCN can exist in two different crystalline forms; the so-called "high temperature" form [21], which is isomorphous with AgCN [26], the chains are parallel and exactly linear, and the "low temperature" form [22] in which the chains contain five crystallography distinct Cu atoms, which form waves with a repeat corresponding to nine CuCN units. These chains are arranged in alternate layers in which the chain axes are rotated by 49° relative to each other. Copper (I) cyanide has shown promise in the assembly of zeolitic-type frameworks [27–30] and as a precursor in the synthesis of $YBa_2Cu_3O_{7-x}$ superconductors [31].

Single crystal studies for a number of CuCN complexes with nitrogen bases have been reported previously [32–39] forming different structure topologies. However, the possibility of obtaining similar arrays with pyridine derivatives has been much less extensively studied, there being as yet no structurally characterized. The form $[(CuCN)_n(L)_m]$ L = pyridine derivatives are a part from the adducts $[Cu_2(CN)_2(4\text{-mpy})_3]$ [35], [CuCN $(py)_2$] [33, 40], $[(CuCN)_2(2\text{-mpy})_3]$ [33]. All the structures of these adducts are single-stranded polymers compressing sequences of copper(I) atoms linked by single end-coordinated cyanides with one or two pyridine ligands appended, with associated copper atom coordination numbers of three or four.

Extending the previous essays, Cu(I)CN : L, L = pyridine (py), 3-methyl pyridine (3-mpy) and 2,4,6-trimethyl-pyridine (tmpy) adducts have been crystallized from H_2O/CH_3CN solution containing Me_3SnCl, three distinct

complexes have been obtained for which single crystals have been isolated for **3** and subjected to single crystals X-ray studies, while **1**, **2** are investigated by IR, mass, and ^{1}H-NMR spectra, as well as TGA.

Experimental section

All chemicals and solvents used in this study were of analytical grade supplied by Aldrich or Merck and used as received except $K_3[Cu(CN)_4]$,which was prepared in the laboratory according to literature [41, 42]. Microanalyses (C, H, N) were carried out with a Perkin Elmer 2400 automatic elemental analyzer. The IR spectra were recorded on Perkin Elmer 1430 Ratio Recording Infrared Spectrophotometer as KBr discs. Mass spectra were recorded on GCMS-Finnigan SSQ 70000. Thermogravimetric analysis was carried out on a Shimadzu AT 50 thermal analyzer (under N_2 atmosphere). ^{1}H NMR spectra were recorded on a Bruker DPX 200 Spectrometer, using deuterated dimethylsulfoxide (DMSO-d_6) as solvent. Electronic absorption spectra as solid matrices were measured on Shimadzu (UV-310PC) spectrometer. Fluorescent spectra as solid matrices were measured with a Perkin Elmer (LS 50 B) spectrometer.

Synthesis of [CuCN·0.5(L)] [L = py, 3-mpy] (**1**, **2**)

A solution of 90 mg (0.31 mmol) of $K_3[Cu(CN)_4]$ in 20 mL H_2O was added, under gentle stirring, to a solution of 189 mg (0.95 mmol) of Me_3SnCl in 15 mL H_2O and 0.2 mL (2.6 mmol) of pyridine (py) **1** or 0.2 mL (2.1 mmol) of 3-methyl pyridine (3-mpy) **2** in 20 mL acetonitrile, already after 1 week a white product of **1** and green crystalline precipitate of **2** were resulted. After filtration, subsequent washing with water and overnight drying, about 30 mg (30% referred to $K_3[Cu(CN)_4]$) of white products **1** or about 29 mg (27.5% referred to $K_3[Cu(CN)_4]$) of green crystalline products **2** were obtained. The crystals of **2** are not good enough for X-ray measurements. Trails to obtain good quality of single crystals of **2** are so currently made, however, they are so far unsuccessful. All attempts for the synthesis of **1** and **2** at room temperature in the absence of Me_3SnCl were unsuccessful.

Anal. Calc. for **1** ($C_7H_5N_3Cu_2$): C, 32.5; H, 1.93; N, 16.27%. Found: C, 32.25; H, 1.8; N, 16.28%.

Anal. Calc. for **2** ($C_8H_7N_3Cu_2$): C, 35.2; H, 2.57; N, 15.4%. Found: C, 35.03; H, 2.8; N, 15.2%.

Synthesis of [CuCN·0.5(tmpy)] (**3**)

Under room temperature, a solution of 90 mg (0.31 mmol) of $K_3[Cu(CN)_4]$ in 30 mL H_2O was added, under gentle stirring, to a solution of 189 mg (0.95 mmol) of Me_3SnCl in 10 mL H_2O and a solution of 0.2 mL (1.5 mmol) 2,4,6-trimethyl pyridine (tmpy), collidine, in 20 mL acetonitrile. Already after week, colorless crystals started growing from the initially clear solution, after filtration, washing with small cold quantity of H_2O and acetonitrile, and overnight drying, about 45 mg (95.7% referred to $K_3[Cu(CN)_4]$ of colorless crystals were obtained. All attempts for the synthesis of **3** at room temperature in the absence of Me_3SnCl were unsuccessful.

Anal. Calc. for **3** ($C_{10}H_{11}N_3Cu_2$): C, 39.97; H, 3.6; N, 14%. Found: C, 39.8; H, 3.5; N, 13.8%.

Single crystal structure determination

Structural measurements for CP **3** was performed on a Kappa CCd Enraf–Nonius FR 90 four circle goniometer with graphite monochromatic MoKα radiation {[λMoKα] = 0.71073 Å} at 25 ± 2 °C. All structures were solved using direct methods and all of the non-hydrogen atoms were located from the initial solution or from subsequent electron density difference maps during the initial stages of the refinement. After locating all of the non-hydrogen atoms in each structure, the models were refined against F^2, first using isotropic and finally using anisotropic thermal displacement parameters. The positions of the hydrogen atoms were then calculated and refined isotropically, and the final cycle of refinements was performed. The cyano groups of all structures are ordered unless otherwise stated. Crystallographic data for CP **3** is summarized in Table 5. Selected bond distances and bond angles are given in Table 6.

Results and discussion

In spite of the presence of Me_3SnCl to produce heterobimetallic CPs, the reactions of the ternary adducts $K_3[Cu(CN)_4]$, Me_3SnCl and L, L = py, 3-mpy and tmpy resulted exclusively in the formation of the tin free assemblies CPs **1**, **2**, **3**. In absence of Me_3SnCl, the reaction does not proceed any more and consequently no product is formed under the used experimental conditions. The presence of Me_3SnCl seems to be essential for the reaction to proceed thermodynamically at room temperature, the point which needs further investigation. However, it is known that the Me_3SnCl molecule has weak Sn···Cl bond, as the non polar trimethyltin(IV) units are bridged to the chlorine atoms by unequal, relatively large, (2.430 and 3.269 Å) distances [43]. In this case, one might suggest that this may cause decomposition of the tetrahedral $[Cu(CN)_4]^{-3}$ anion to different $(Cu)_n(CN)_m$ fragments, which are readily assembled with the other reactants in solution to produce the thermodynamically more stable coordination polymer.

The Me_3SnCl may form, in this case, the more stable Me_3SnCN, as the Sn–C or the Sn–N bond distances of the ordered C–N–Sn–N–C or even N–C–Sn–C–N chains are in the range of 2.49 ± 0.02 Å or may form the $(Me_3Sn)_2$ dimer [44, 45]. There are two abnormal features in these reactions that they are formed at room temperature producing significant amounts of single-phase products and resulted exclusively in the formation of the tin free assembly **1**, **2**, **3** rather than to produce, as was expected, zeolitic-type CPs.

Infrared spectra

The IR spectra of CPs **1–3** exhibit the characteristics bands of the $(CuCN)_n$ fragment and the unidentate pyridine bases. The IR spectra showed strong bands, whose frequencies along with those reported else where [22, 33, 46–48] are given in Table 1. The $\nu_{C\equiv N}$ bands of the CPs **1–3** locate at 2,115, 2,119, and 2,117 cm^{-1}, respectively, which are higher than the bands of the genuine salts of the corresponding $[M(CN)_n]^{m-}$ anions [48]. The stretching frequencies much higher than those of the genuine salt have been assigned to linear bridging between centers, Cu–CN–Cu, while frequencies near these of the salt are associated with terminal or nonlinearly bridging cyanide groups [49]. In this concept, solid CuCN contains extended linear –CuCN–CuCN– chains with $\nu_{C\equiv N} = 2{,}172\ cm^{-1}$ [22]. Thus, the $\nu_{C\equiv N}$ frequencies of the CPs **1–3** are higher than that of $K_3[Cu(CN)_4]$ [47] and lower than those of CuCN and $[(^nBu_4N)Cu(CN)_2]$ [46], a result of the fact that the $(CuCN)_n$ chains in the structures of the CPs **1–3** are nonlinear containing bridging cyanide groups. This is further supported by the fact that the frequencies of the $\nu_{C\equiv N}$ appear at more or less the same position of the prototype compounds $[(CuCN)_2(2\text{-mpy})_3]$ [33], $[Cu_2(CN)_2(4\text{-mpy})_3]$ [35], [CuCN $(py)_2$] [33], Table 1.

The stretching vibrations of Cu–C bond appear as a weak band at 455, 462, and 472 cm^{-1} in the IR spectra of the CPs **1**, **2**, and **3**, respectively, supporting the presence of the $(CuCN)_n$ fragments. A downward frequency shift is observed for the $(\nu_{(CuC/N)})$ mode than that observed for CuCN or even for $CuCN{:}NEt_3$ ($\nu_{(CuC} = 531\ cm^{-1}$) [33] due to the binding of the pyridine ligands to the copper(I) atom which weakens the Cu–C/N bonds.

The IR spectra of the CPs **1–3** display the characteristics bands of the unidentate pyridine bases. The bands at 3,030–3,095 cm^{-1} are attributed to $\nu_{CH(arom.)}$ in the CPs **1–3**. The bands at 2,847–2,970 cm^{-1} correspond to $\nu_{CH(aliph.)}$ in the CPs **2**, **3**. Furthermore, the bands at 1,617–1,585, 1,650–1,519, and 1,469–1,444 cm^{-1} are due to $\nu_{C=N}$ and $\nu_{C=C}$ of the ligands in the CPs **1–3**, respectively, Table 2.

Table 1 The $\nu_{(C\equiv N)}$ and $\nu_{(CuC/N)}$ vibrational frequencies in cm^{-1} of some Cu(I) cyanides

Compound	Chain type	$\nu_{(C\equiv N)}$	$\nu_{(CuC/N)}$	Strc. refer.
CuCN	Linear	2172	591	[22]
$[(^nBu_4N)Cu(CN)_2]$	Linear	2190, 2210	–	[46]
$K_3[Cu(CN)_4]$	Non-bridged	2076	–	[47]
$[(^nBu_4N)_3Cu(CN)_4]$	Non-linear	2082, 2076	–	[48]
$[(CuCN)_2(2\text{-mpy})_3]$	Non-linear	2116	[a]	[33]
$[Cu_2(CN)_2(4\text{-mpy})_3]$	Non-linear	2114	[a]	[35]
[CuCN $(py)_2$]	Non-linear	2105	–	[33]
$[(CuCN)_2(py)]$	Non-linear	2115	455	This work
$[(CuCN)_2(3\text{-mpy})]$	Non-linear	2119	462	This work
$[(CuCN)_2(tmpy)]$	Non-linear	2105	460	This work

[a] Obscured by strong bands due to the coordinated ligand

Thermogravimetric analysis

The thermogram of the CP **1**, Fig. 1, shows two steps. The first step is at 70–250 °C, corresponding to the release of the py ligand as well as one cyanide group. At 250–520 °C, the weight loss is due to the decomposition of the other cyanide group. On the other hand the thermogram of the CP **2**, Fig. 1, shows two interfering steps at 80–340

Table 2 The wavenumbers (cm^{-1}) of different vibrational modes of the CPs **1–3**

No.	Compound	$\nu_{(CH)}$ (arom)	$\nu_{(CH)}$ (aliph)	$\nu_{(C\equiv N)}$	$\nu_{(C=N)}$ and $\nu_{(C=C)}$ (arom.)	Skeletal and C–C vibrs. of L	δ_{CH} of L	γ_{CH} of L	$\nu_{(Cu-C)}$
1	[CuCN·0.5 (py)]	3095m	–	2164m	1591s	1234m–1191m	1364m	732s	455w
		3030m		2115s	1519s–1469s	1156m–1034m		664s	
2	[CuCN·0.5 (3-mpy)]	3091w	2970m	2157m	1585s	1235m–1189s	1418s	789s	462w
		3045m	2913w	2119s	1546s–1444s	1112s–1042s		581s	
3	[CuCN·0.5(tmpy)]	3050m	2943m	2122s	1617s–1560s	1236s–1028s	1375m	852m	472w
			2847m	2082w	1455s			725w	
				2039w					

s strong, *m* medium, *w* weak

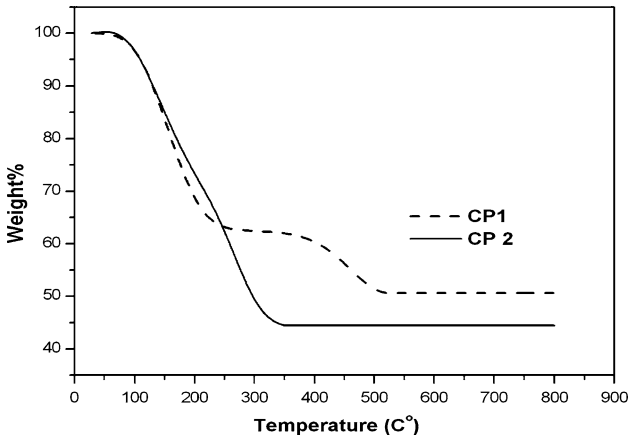

Fig. 1 Thermogravimetric analysis of the CPs **1**, **2**

corresponding to the total mass loss, which is due to the decomposition of 3-mpy ligand as well as two cyanide groups. The molecular weights of the residues obtained after complete thermolysis of the CPs **1**, **2** are coincident with metallic copper.

The thermogravimetric analysis of the CPs **1**, **2** indicated the presence of the CuCN fragment as well as the pyridine ligands as basic units for construction of their structures. These structures are stable on expose to air up to 100 °C where above this temperature the release of unidentae pyridine ligands takes place.

^{1}H-NMR spectra

The ^{1}H-NMR spectrum of the CP **1** shows three broad bands at 7.6, 7.9, and 8.7 ppm that are assigned to the three different protons of the pyridine ring. However, the ^{1}H-NMR spectrum of the CP **2** shows one broad band at 7.99 ppm corresponding to the aromatic protons of 3-mpy. The methyl protons of 3-mpy in CP **2** display a strong singlet band at 2.5 ppm, which interfere with the band of DMSO protons.

The absence of the band at 0.47–0.49 ppm [48], due to $(Me_3Sn)^+$ cation in the ^{1}H-NMR spectra of the CPs **1**, **2** is good evidence of the formation of tin free compounds.

Mass spectra

The constitution and purity of the CPs **1**, **2** are established by mass spectrometry. The mass spectrum of CP **1**, Table 3, exhibits the peak at *m/z* 79 corresponding to the molecular ion of pyridine (py). Also it shows the ion peaks at *m/z* 89, 91, *m/z* 105, *m/z* 126, 130, *m/z* 152, 156, *m/z* 178, 182, *m/z* 241, 247, *m/z* 267, 273, *m/z* 330, 338, and *m/z* 356, 364 corresponding to $[Cu^{63}CN]^+$, $[Cu^{65}CN]^+$, $[CN\ (py)]^+$, $[2Cu^{63}]^+$, $[2Cu^{65}]^+$, $[(Cu^{63})_2CN]^+$, $[(Cu^{65})_2CN]^+$, $[(Cu^{63})_2(CN)_2]^+$, $[(Cu^{65})_2(CN)_2]^+$, $[(Cu^{63})_3(CN)_2]^+$, $[(Cu^{65})_3(CN)_2]^+$, $[(Cu^{63})_3(CN)_3]^+$, $[(Cu^{65})_3(CN)_3]^+$, $[(Cu^{63})_4(CN)_3]^+$, $[(Cu^{65})_4(CN)_3]^+$ and $[(Cu^{63})_4(CN)_4]^+$, $[(Cu^{65})_4(CN)_4]^+$, respectively. On the other hand, the ion peaks located at *m/z* 142, 144, *m/z* 168, 170, *m/z* 205, 209, and *m/z* 284, 288 are attributed to $[Cu^{63}(py)]^+$, $[Cu^{65}(py)]^+$, $[Cu^{63}CN{\cdot}(py)]^+$, $[Cu^{65}CN{\cdot}(py)]^+$, $[(Cu^{63})_2(py)]^+$, $[(Cu^{65})_2(py)]^+$, and $[(Cu^{63})_2(py)_2]^+$, $[(Cu^{65})_2(py)_2]^+$, respectively. Also, the mass spectrum of CP **1** shows the ion peaks at *m/z* 310, 314, *m/z* 336, 340, and *m/z* 346, 352 corresponding to $[(Cu^{63})_2(CN).(py)_2]^+$, $[(Cu^{65})_2(CN).(py)_2]^+$, $[(Cu^{63})_2(CN)_2.(py)_2]^+$, $[(Cu^{65})_2(CN)_2.(py)_2]^+$, and $[(Cu^{63})_3(CN)_3\ (py)]^+$, $[(Cu^{65})_3(CN)_3.(py)]^+$, respectively. Furthermore, the mass spectrum of CP **1** exhibits the molecular ion peak at *m/z* 257, 261 corresponding to $[(Cu^{63})_2(CN)_2(py)]^+$, $[(Cu^{65})_2(CN)_2(py)]^+$.

Table 3 Interpretation of the mass spectrum of [CuCN·0.5(py)] **1**

m/z	Ion	*m/z*	Ion
51	$[C_4H_3]^+$	205	$[(Cu^{63})_2(py)]^+$
79	$[C_5H_5N]^+$	209	$[(Cu^{65})_2(py)]^+$
89	$[Cu^{63}CN]^+$	241	$[(Cu^{63})_3(CN)_2]^+$
91	$[Cu^{65}CN]^+$	247	$[(Cu^{65})_3(CN)_2]^+$
105	$[CN{\cdot}(py)]^+$	257	$[(Cu^{63})_2(CN)_2(py)]^+$ = M.W
126	$[2Cu^{63}]^+$	261	$[(Cu^{65})_2(CN)_2(py)]^+$ = M.W
130	$[2Cu^{65}]^+$	267	$[(Cu^{63})_3(CN)_3]^+$
142	$[Cu^{63}(py)]^+$	273	$[(Cu^{63})_3(CN)_3]^+$
144	$[Cu^{65}(py)]^+$	284	$[(Cu^{63})_2(py)_2]^+$
152	$[(Cu^{63})_2CN]^+$	288	$[(Cu^{65})_2(py)_2]^+$
156	$[(Cu^{65})_2CN]^+$	310	$[(Cu^{63})_2(CN).(py)_2]^+$
168	$[Cu^{63}CN{\cdot}(py)]^+$	314	$[(Cu^{65})_2(CN).(py)_2]^+$
170	$[Cu^{65}CN{\cdot}(py)]^+$	346	$[(Cu^{63})_3(CN)_3.(py)]^+$
178	$[(Cu^{63})_2(CN)_2]^+$	352	$[(Cu^{65})_3(CN)_3.(py)]^+$
182	$[(Cu^{65})_2(CN)_2]^+$	330	$[(Cu^{63})_4(CN)_3]^+$
356	$[(Cu^{63})_4(CN)_4]^+$	338	$[(Cu^{65})_4(CN)_3]^+$
364	$[(Cu^{65})_4(CN)_4]^+$	336	$[(Cu^{63})_2(CN)_2.(py)_2]^+$
		340	$[(Cu^{65})_2(CN)_2.(py)_2]^+$

The mass spectrum of CP **2**, Table 4, exhibits the peak at *m/z* 93 corresponding to the molecular ion of 3-methylpyridine (3-mpy). Fragmentation of 3-mpy ion gives rise to peaks at *m/z* 92, *m/z* 78, *m/z* 66, and *m/z* 51 due to $[C_6H_6N]^+$, $[C_5H_4N]^+$, $[C_5H_5]^+$, and $[C_4H_3]^+$, respectively. Furthermore, the mass spectrum of CP **2** shows the ion peaks at *m/z* 63, 65, *m/z* 89, 91, *m/z* 126, 130, *m/z* 152,156, and *m/z* 178, 182 corresponding to $[Cu^{63}]^+$, $[Cu^{65}]^+$, $[Cu^{63}CN]^+$, $[Cu^{65}CN]^+$, $[2Cu^{63}]^+$, $[2Cu^{65}]^+$, $[(Cu^{63})_2CN]^+$, $[(Cu^{65})_2CN]^+$, and $[(Cu^{63})_2(CN)_2]^+$, $[(Cu^{65})_2(CN)_2]^+$, respectively. On the other hand, the ion peaks appearing at *m/z* 156, 158 and *m/z* 182, 184 are attributed to $[Cu^{63}(3\text{-mpy})]^+$, $[Cu^{65}(3\text{-mpy})]^+$ and $[Cu^{63}CN\ (3\text{-mpy})]^+$, $[Cu^{65}CN\ (3\text{-mpy})]^+$, respectively. Also, the mass spectrum of CP **2** exhibits the molecular ion peak at m/z 273, 275

Table 4 Interpretation of the mass spectrum of [CuCN·0.5(3-mpy)] **2**

m/z	Ion	*m/z*	Ion
51	$[C_4H_3]^+$	152	$[(Cu^{63})_2CN]^+$
63	$[Cu^{63}]^+$	156	$[(Cu^{65})_2CN]^+$
65	$[Cu^{65}]^+$	156	$[Cu^{63}(3\text{-mpy})]^+$
66	$[C_5H_5]^+$	158	$[Cu^{65}(3\text{-mpy})]^+$
78	$[C_5H_4N]^+$	178	$[(Cu^{63})_2(CN)_2]^+$
89	$[Cu^{63}CN]^+$	182	$[(Cu^{65})_2(CN)_2]^+$
91	$[Cu^{65}CN]^+$	182	$[Cu^{63}CN\ (3\text{-mpy})]^+$
92	$[C_6H_6N]^+$	184	$[Cu^{65}CN\ (3\text{-mpy})]^+$
93	$[3\text{-mpy}]^+$	273	$[(Cu^{63})_2(CN)_2(3\text{-mpy})]^+ = M.W$
126	$[2Cu^{63}]^+$	275	$[(Cu^{65})_2(CN)_2(3\text{-mpy})]^+ = M.W$
130	$[2Cu^{65}]^+$		

corresponding to $[(Cu^{63})_2(CN)_2.(3\text{-mpy})]^+$, $[(Cu^{65})_2(CN)_2(3\text{-mpy})]^+$.

Thus, the mass spectra of the CPs **1**, **2** confirm the presence of the unidentate pyridine ligand and the CuCN fragments, and support the polymeric nature of the (CuCN) building blocks. Also, they confirm the molecular formula of the CPs **1** and **2**.

Crystal structure of [CuCN·0.5(tmpy)] **3**

The asymmetric unit of the CP **3** confirms the assignment of 2:1 stoichiometry for the copper(I)-cyanide:trimethylpyridine adduct, with one crystallographically copper(I) atom, one ordered cyanide group and half ligand molecule, Fig. 2. Crystallographic data for CP **3** is summarized in Table 5. Selected bond distances and bond angles are given in Table 6. The X-ray analysis reveals that the structure of the CP **3** displays 1D-extended chain of $(CuCN)_n$ with tmpy attached to every Cu atom, which exhibits a distorted trigonal planer site. The angles of the trigonal structure deviate largely than being 120° in spite of the fact that the sum of the angles is 360°, due to the pyramidization of the

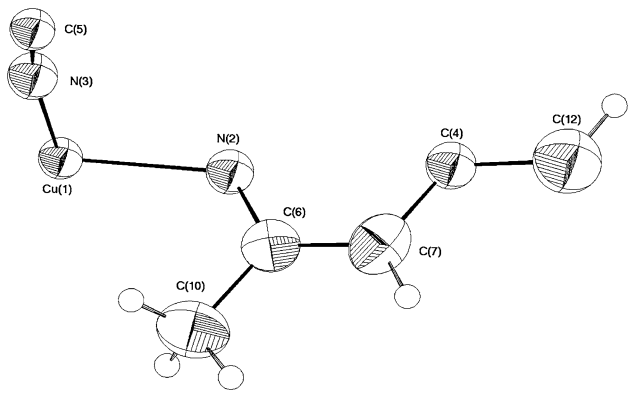

Fig. 2 An ORTEP plot of the asymmetric unit of the CP **3** with atom labeling scheme

Table 5 Crystal data for the CP **3**

Empirical formula	$C_{10}H_{11}Cu_2N_3$
Formula weight (g/mol)	300.082
Temperature (K)	298
Crystal system	Orthorhombic
Space group	Pnma
a (Å)	9.1065 (3)
b (Å)	8.6669 (3)
c (Å)	12.1998 (5)
α (°)	90.00
β (°)	90.00
γ (°)	90.00
V (Å^3)	962.87 (6)
Z	8
μ(Mo-Kα)/m m^{-1}	4.40
Calculated density/g cm^{-3}	2.355
Goodness-of-fit on F^2	1.269
F(000)	956
R indices[$I > 3\sigma(I)$] *R*1/*wR*2	0.035/0.084
R indices(all data)	0.054/0.086
R_{int}	0.021
Data/restraints/parameters	872/0/64

Table 6 Bond lengths (Å) and bond angles (°) of CP **3**

Cu1–N2	2.070 (3)	Cu1–C6^{i}	2.961 (3)
Cu1–N2^{i}	2.070 (3)	Cu1–Cu1^{iii}	4.9430 (3)
Cu1–N3	1.961 (3)	Cu1–Cu1^{ii}	4.9430 (3)
N3–C5	1.131 (5)	Cu1–N3^{iii}	3.005 (3)
Cu1–N3^{i}	1.961 (3)		
Cu1–C5^{ii}	1.875 (4)	N2–Cu1–N3	96.70 (12)
Cu1–C5^{iii}	1.875 (4)	N2–Cu1–C5^{ii}	130.56 (14)
C10–H10A^{i}	3.147 (2)	N3–Cu1–C5^{ii}	132.7 (2)
Cu1–N3^{ii}	3.005 (3)	Cu1^{i}–N3–C5	170.3 (3)
Cu1–C10^{i}	3.097 (3)	Cu1–N2–C6	119.68 (14)

Symmetry codes: (i) $x - 1$, $1/2 - y$, $1/2 + z$; (ii) $x - 1 - x$, $1/2 + y$, $3/2 - z$, (iii) $x - 1/2$, $1/2 - y$, $1/2 - z$

trigonal structure around the Cu atoms which is caused by close Cu–C contacts of the pyridine ring and Cu1–C contacts of the methyl groups in the tmpy ligand; Cu1–C6 = 2.961(3) Å, Cu–C10 = 3.097(3) Å, and the great crowdness of the three methyl groups of the tmpy ligand.

Alternatively, the structure of the CP **3** consists of $(CuCN)_n$ building blocks, which are connected by the CN group forming 1D-zig-zag chain, while the tmpy ligands alternate on both sides of the chain upwards and downwards. The cyanide groups in the CP **3** exhibit the usual bond length of 1.072–1.177 Å, while the Cu1–N3 bond length is 1.961 Å and the Cu–N(tmpy) bond length is 2.070 Å, which all are in the usual range reported for the

prototype compounds [32–39]. The 1D-zig-zag chain is weakly bonded to another chain by hydrogen bonding between the carbon of the methyl group in the tmpy ligand in one chain and the hydrogen atom of the methyl group in the tmpy ligand in another chain, developing two-dimensional sheet (C10–H10A bond length is 3.147 Å), Fig. 3.

The X-ray single crystal determination shows that the structure of the CP **3** has a single stranded polymer Cu(CN)Cu(CN) spine, being propagated along the *c*-axis, by inversion centers located at the CN bond centers, and translations, the ligands disposed to either side of the chain, interleaving with adjacent polymer strands and overlapping with inversion related equivalents. Furthermore, the extended structure of the CP **3** is a 2D-fishbone like structure, which is formed via H-bonding and Cu–C contacts, Fig. 4 and Table 6.

It is worth mentioned that there is no any kind of hydrogen bonding interactions or π–π stacking between the fragments of the main building blocks. Also, there is no any kind of π–π stacking interactions between the fragments of the adjacent chains. However, in spite of the shape of the structure of the main building blocks down the projection of the *c*-axis, looks like a rectangle open shape; 8.006 Å × 5.619 Å with Cu–Cu distance equals to 8.006 Å, Fig. 4, the CP **3** forms an open framework at the methyl groups of the tmpy ligand along any other axes and creates hexagonal cavities; 11.024 Å × 6.680 Å. The shortest distance between two Cu1 atoms in these presented hexagonal cavities is 6.680 Å. There is no Cu–Cu interaction, as the shortest distances between Cu1–Cu1 = 4.9430 Å.

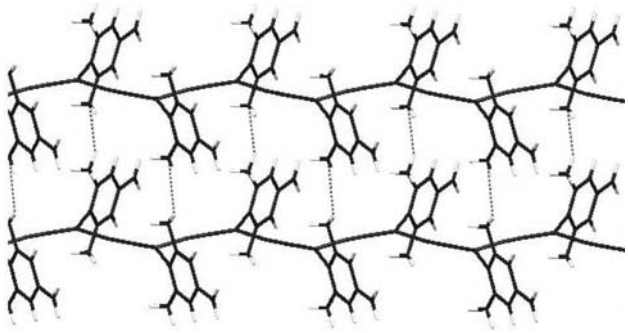

Fig. 3 A view of the hydrogen bonds between two adjacent chains along the *a*-axis in the CP **3**

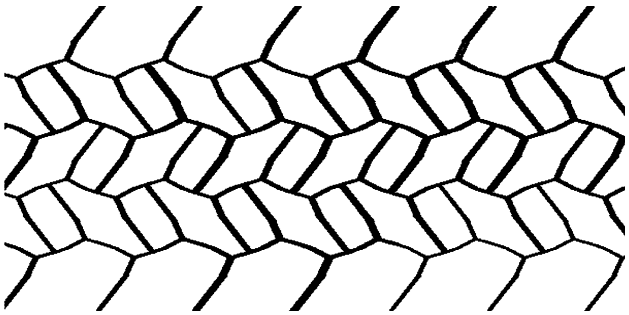

Fig. 4 The 2D-rectangle open framework structure of the CP **3** along the *c*-axis. H-atoms have been omitted for clarity

Electronic absorption and emission spectra of the CPs **1–3**

The electronic absorption spectra of the CPs **1–3** display absorption bands at 255, 280–295, 315, and 345–355 nm, while in the case of the CP **2** an additional broad band is observed at 450 nm. The high energy band at 255 nm corresponds to ^1L_b transition in pyridine, which is due to $^1B_1 \leftarrow {}^1A$ transition and is allowed. The methyl group produces a slight red shift in the spectra of the CPs **2** and **3.** The remaining bands around 290, 315, and around 350 nm resembles these observed in the spectrum of copper cyanide. The bands in the region of 280–315 nm show prominent vibrational structure in the case of CuCN and the CP **2** while they are much less prominent in the case of the CPs **1** and **3**. They correspond to metal-to-ligand charge transfer (MLCT), which the band at 345–355 nm is due to π–π^* transitions of the cyanide ligand. Thus, the resemblance of the absorption spectra of the CPs **1–3** and that of the CuCN indicates that the structure of the CPs **1–3** is mainly constructed of corrugated CuCN chains, which are arranged in alternate layers. On the other hand, no band due to n–π^* transitions is observed in the spectra of the CPs **1–3** supporting the coordination of py, 3-mpy, and tmpy as well as the cyanide ligand to the copper atom via the lone pair of electrons of the nitrogen atoms. The long wavelength band at 450 nm observed in the spectrum of the CP **2** is due to intermolecular charge transfer from 3-mpy to the copper atom (LMCT).

The emission spectra of the CPs **1–3** display structural bands centered at 445–460, 480–490, and 525 nm, Fig. 5.

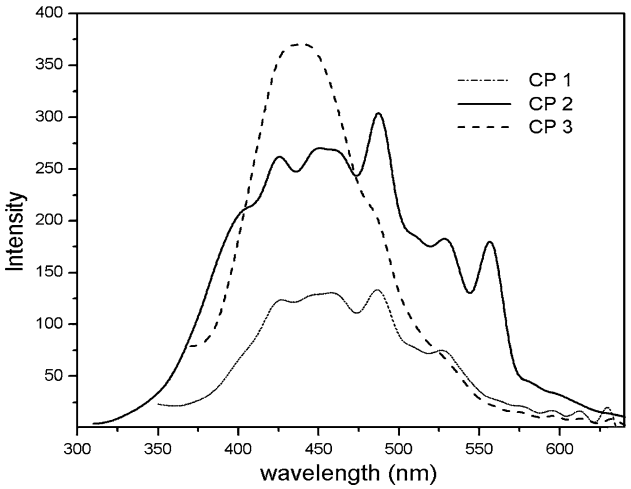

Fig. 5 Solid-state emission spectra of the CPs **1–3** upon excitation at 330 nm

Usually, py and its derivatives exhibit very weak luminescence [50], however, the CPs **1–3** exhibit strong fluorescence behavior. The emission band centered at 445–460 nm corresponds to the lowest π–π^* state in the ligand. The emission bands at 480–490 and 525 nm may be attributed to MLCT or metal centered transitions of the type $3d^{10} \rightarrow 3d^9\ 4s^1$ and $3d^{10} \rightarrow 3d^9\ 4p^1$ on the Cu(I) center.

Conclusion

The results reinforce the observation that the cyanide group is an effective bridging ligand, which can link together two copper centers; μ_2–**1**, **2**–CN. The cyanide group is popular bridging one for construction of the solid-state structures, and appears to be a potentially useful synthon for crystal engineering. The presence of Me_3SnCl has an important role for the synthesis of copper(I) cyanide CPs at room temperature in spite of the fact that the CPs **1–3** are tin free. The stoichiometry of the CPs **1–3** is 2:1 [$(CuCN)_2$:L], which is different than those of the prototype compounds containing py, 2-mpy, or 4-mpy. These compounds are richer in the unidentate pyridine ligands than the CPs **1–3**, that the copper atom is four coordinated to two cyanide units and two unidentate pyridine ligands. On the other hand, the CuCN complexes containing 2.2′-bipyridine or 2,6-bis (1,2,4-triazolyl)pyridine (btp) exhibit 3D-metal organic framework via Cu···Cu, π–π stacking, and the tridentate btp, respectively [36]. The CPs **1–3** are 2D-polymers comprising puckered CuCN chains with one unidentate ligands appended, with associated copper atom coordination number of three. Hydrogen bonds play an essential role for developing 2D-network structure.

Supplementary material

CCDC 721591 contains the supplementary crystallographic data for **3**. This data can be obtained free of charge via http://www.ccdc.cam.ac.uk/conts/retrieving.html, or from the Cambridge Crystallographic Data Centre, 12 Union Road, Cambridge CB2 1EZ, UK; fax: (+44) 1223-336-033; or e-mail: deposit@ccdc.cam.ac.uk.

References

1. Ockwig NW, Friedrichs OD, O'keeffe M, Yaghi OM (2005) Acc Chem Res 38:176
2. Kitagawa S, Kiteura R, Nora SI (2004) Angew Chem Int Ed 116:2388
3. James SL (2003) Chem Soc Rev 32:276
4. Janiak C (2003) J Chem Soc Dalton Trans 2781
5. Zheng SL, Chen XM (2004) Aust J Chem 57:703
6. Georgiev IG, MacGillivray LR (2007) Chem Soc Rev 36:1239
7. Sherrington DC, Taskinen KA (2001) Chem Soc Rev 30:83
8. Colacio E, Kivekas R, Lloret F, Sunberg M, Varela JS, Bardaji M, Laguna A (2002) Inorg Chem 41:5141
9. Vera JMD, Moreno JM, Colacio E (2004) Inorg Chim Acta 357:611
10. Liang SW, Li MX, Shao M, Miao ZX (2006) Inorg Chem Commun 9:1312
11. He X, Lu CZ, Yuan DQ, Chen SM, Chen JT (2005) Eur J Inorg Chem 11:2181
12. He X, Lu CZ, Wu CD, Chen LJ (2006) Eur J Inorg Chem 12:2491
13. Chestnut DJ, Kusnetzow A, Birge RR, Zubieta J (1999) Inorg Chem 38:2663
14. Chesnut DJ, Zubieta J (1998) Chem Commun 1707
15. Liang S-W, Li M-X, Shao M, He X (2008) J Mol Struct 17:875
16. Wang H, Li M-X, Shao M, He X (2007) Polyhedron 26:5171
17. Tronic TA, deKrafft KE, Lim MJ, Ley AN, Pike RD (2007) Inorg Chem 46:8897
18. Chi Y-N, Cui F-Y, Xu Y-Q, Hu C-W (2007) Eur J Inorg Chem 4375
19. Bowmaker GA, Kenncdy BJ, Reid JC (1998) Inorg Chem 37:3968
20. Krocker S, Wasylishen RE, Hanna JV (1999) J Am Chem Soc 121:1582
21. Hibble SJ, Cheyne SM, Hannon AC, Eversfield SG (2002) Inorg Chem 41:4990
22. Hibble SJ, Eversfield SG, Cowley AR, Chippindale AM (2004) Angew Chem Int Ed 43:628
23. Reckeweg O, Lind C, Simon A, Disalvo FJ (2003) Z Naturforsch 58:155
24. Wang J, Collins MF, Johari GP (2002) Phys Rev B65:180103
25. Wang J, Johari GP (2003) Phys Rev B68:214201
26. Hibble SJ, Cheyne SM, Hannon AC, Eversfield SG (2002) Inorg Chem 41:1042
27. Hoskins BF, Robson R (1990) J Am Chem Soc 112:1546
28. Brimah AK, Siebel E, Fischer RD, Davies NA, Apperley DC, Harris RK (1994) J Organomet Chem 475:85
29. Brousseau LC, Williams D, Kouvetakis J, O'Keefe M (1997) J Am Chem Soc 119:6292
30. Zhang C, Jin G, Xu Y, Fun H-K, Xin X (2000) Chem Lett 502
31. Khan NA, Baber N, Zafar Iqbal M, Mazhar M (1993) Chem Mater 5:1283
32. Bowmaker GA, Pettinari C, Skelton BW, Somers N, Vigar NA, White AH (2007) Z Anorg Allg Chem 633:415
33. Bowmaker GA, Lim KC, Skelton BW, White AH (2004) Z Naturforsch 59b:1264
34. Bowmaker GA, Lim KC, Skelton BW, White AH (2004) Z Naturforsch 59b:1293
35. Dyason JC, Healy PC, Engelhardt LM, Pakawatchai C, Patrick VA, White AH (1985) J Chem Soc Dalton Trans 839
36. Liang S-W, He X, Shao M, Li M-X (2008) J Coord Chem 61:2999
37. Yao Z-F, Gan X, Fu W-F (2009) J Coord Chem 62:1817
38. Massoud AA, Langer V, Thrstrom L, Morsy AM, Abu-Youssef (2009) J Coord Chem 62:519
39. Zhai Q-G, Niu J-P, Hu M-C, Wang Y, Ji W-J, Li S-N, Jiang Y-C (2009) J Coord Chem 62:2927
40. Olmstead MM, Speier G, Szabö L (1993) Acta Crystallogr Sect 49:370
41. Eastes JW, Burgess WM (1942) J Am Chem Soc 64:1187
42. Eastes JW, Burgess WM (1942) J Am Chem Soc 64:2715
43. Lefferts JL, Molly KC, Hossain MB, Vander Helen D, Zuckerman JJ (1982) J Organomet Chem 240:349
44. Avalle P, Harris RK, Hanika-Hiedl H, Dieter Fisher R (2004) Solid State Sci 6:1069

45. Etaiw SEH, Amer SA, El-bendary MM (2009) Polyhedron 28:2385
46. Nilson M (1982) Acta Chem Scand B36:125
47. Penneman RA, Jones LH (1956) J Chem Phys 24:293
48. Ibrahim AMA (1998) J Organomet Chem 556:1
49. Bonardi A, Corini C, Pelizzi C, Pelizzi G, Predieri G, Torasconi P (1991) J Organomet Chem 401:283
50. Valeur B (2002) Molecular fluorescence principles and applications, Wiley-VCH Verlag GmbH, Weinheim, p 59